J. Chem. Chem. Eng. 10 (2016) 153-160
doi: 10.17265/1934-7375/2016.04.001

Novel Synthesis Method of Nonstoichiometric $Na_{2-x}IrO_3$ Crystal Structure, Transport and Magnetic Properties

Katharina Rolfs*[1], Ekaterina Pomjakushina[1], Denis Sheptyakov[2] and Kazimierz Conder[1]

1. Laboratory for Scientific Development and Novel Materials, Paul Scherrer Institute, Villigen PSI, 5232 Switzerland

2. Laboratory for Neutron Scattering and Imaging, Paul Scherrer Institute, Villigen PSI, 5232 Switzerland

Abstract: Transition metal oxides with 4d or 5d metals are of great interest due to the competing interactions, of the Coulomb repulsion and the itineracy of the d-electrons, opening a possibility of building new quantum ground states. Particularly the 5d metal oxides containing Iridium have received significant attention within the last years, due to their unexpected physical properties, caused by a strong spin orbit coupling observed in Ir(IV). A prominent example is the Mott-insulator Sr_2IrO_4. Another member of this family, the honeycomb lattice compound Na_2IrO_3, also being a Mott-insulator having, most probably, a Kitaev spin liquid ground state. By deintercalating sodium from Na_2IrO_3, the authors were able to synthesize a new honeycomb lattice compound with more than 50% reduced sodium content. The reduction of the sodium content in this layered compound leads to a change of the oxidation state of iridium from + IV to + V/+ VI and a symmetry change from *C2/c* to *P-3*. This goes along with significant changes of the physical properties. Besides the vanishing magnetic ordering at 15 K, also the transport properties changes and instead insulating semiconducting properties are observed.

Key words: Strongly correlated electron systems, iridates, oxidation, neutron diffraction

1. Introduction

In the field of strongly correlated electron systems significant attention has been drawn to 4d and 5d based TMO (transition metal oxides). The SOC (spin orbit coupling) observed in these systems becomes non-negligible and leads to new exotic ground states, such as the Mott insulating state in Sr_2IrO_4 [1]. The interest is focused, among others, on Mott insulators with properties approaching a metal-insulator transition. It was suggested that a spin liquid ground state can be found in such compounds, which farther can lead to new phases, with interesting electronic properties such as high-T_c superconductivity in cuprates [2]. Several iridates, like Na_2IrO_3 and Li_2IrO_3, have been discovered to be quantum frustrated Mott insulators [3]. In these compounds, the SOC is the compelling property, which stabilizes the insulating state even though the onsite Coulomb interactions are relatively weak. Another interesting attribute of Na_2IrO_3 is its honeycomb structure [4, 5], enabling the realization of the exactly solvable spin model with spin liquid ground state proposed by Kitaev [6]. It was suggested that these materials contain the necessary anisotropic exchange interactions (J_K) and that the spin liquid ground state resists the small but always present isotropic exchange (J) [7]. However Na_2IrO_3 and Li_2IrO_3 order magnetically at 15 K, even though this transition temperature is low compared to the characteristic exchange energy [8]. To access the spin liquid phase, the reduction of these isotropic Heisenberg terms or the increase of the anisotropic interactions is necessary. Reuther et al. [7] suggested that the reduction of the chemical pressure along the c-axis can increase J_K and therefore induces the spin glass behavior. This can be achieved either by exerting pressure in the *ab*-plane or substituting Na by smaller Li-ions. Another possible chemical modification of Na_2IrO_3 is a hole doping. This was predicted to lead to a topological superconductivity

Corresponding Author: Katharina Rolfs, Ph.D., main research field: solid state chemistry.

and a Fermi liquid behavior in the vicinity of the Kitaev spin liquid phase [8, 9]. However, the only way to introduce holes into Na_2IrO_3 is introducing sodium deficiency. The direct synthesis of $Na_{2-x}IrO_3$, would result in a mixture of IrO_2 and Na_2IrO_3. As shown by Takeda et al. [10] for $Na_{0.7}CoO_2$, it is possible to oxidize the material by deintercalating the sodium positioned in between the CoO_2 layers. Applying the same chemical oxidation process, it was also possible to oxidize the layered compound Na_2IrO_3 to $Na_{0.8}IrO_3$. Here the authors will show a crystallographic study of this new compound, accompanied by magnetization and transport measurements, showing the significant influence of the change of sodium stoichiometry on physical properties.

2. Experimental

Polycrystalline Na_2IrO_3 was synthesized by a solid state reaction using Na_2CO_3 and IrO_2. A stoichiometric mixture of both powders was heated at 900 °C for 48 h. To ensure a clean compound, the product has been measured by XRD (X-ray diffraction) at room temperature using a Bruker D8 diffractometer in Bragg Brentano Geometry with Cu Kα radiation.

The Na_2IrO_3 powder was added to a Br_2/CH_3CN-solution for 6 h, 24 h and 48 h and subsequently rinsed with water. The dry product was studied by TG/DTA (Thermal Analysis) equipped with mass spectrometer. With these, thermal stability of the compound could be checked and possible phase transitions above room temperature detected. The crystallographic structure was determined by the neutron powder diffraction at 50 K and 2 K with wavelength λ = 1.49 Å at the High Resolution Powder Diffractometer HRPT [11] at SINQ, PSI in Switzerland. The magnetic properties were measured at a Quantum Design MPMS (Magnetic Property Measurement System), the resistivity and heat capacity measurements were done using the PPMS (Physical Property Measurement System).

3. Result and Discussion

3.1 Structural Change and Thermal Stability, Crystal Water

Room temperature XRD measurements of Na_2IrO_3 samples, chemically oxidized for 6 h, 24 h and 48 h are showing very similar pattern which is clearly different from those observed for the parent phase Na_2IrO_3. The diffraction patterns could be indexed in a trigonal unit cell by DICVOL04 with the lattice constants for the sample deintercalated for 24 h, a = 5.230 Å and c = 4.848 Å. The lattice constants for the samples deintercalated for 6 h and 48 h are very similar, as it can be seen in Table 1. Using the Rietveld refinement method, the space group of all three specimens was determined as *P-3* instead of the monoclinic *C2/c* symmetry of the parental phase Na_2IrO_3 [5]. Furthermore, the refinement revealed a significant change in the Na-concentration in the samples from Na_2IrO_3 to approximately $Na_{0.8}IrO_3$. However, the amount of sodium removed from the compounds appears to be independent of the time interval of deintercalation chosen here, since all three specimens shown very similar stoichiometry (Table 1). The sample, deintercalated for 24 h was also measured by neutron diffraction at 2 K and 50 K (Fig. 1), showing no structural phase transition on cooling down to 2 K. Structure refinement could be made with a very high quality as obtained R_f—factors, $R_F = 100\frac{\sum_h|'F_{obs,k}'-F_{calc,h}|}{\sum_h|'F_{obs,h}'|}$, of 4.81 for the neutron data at 2 K, and 3.72 at 50 K are showing. The

Table 1 Stoichiometry, cell parameters and R_f factor of Rietveld refinement of $Na_{2-x}IrO_3$ deintercalated for 6 h, 24 h and 48 h.

Time [h]	Stoichiometry	a [Å]	c [Å]	R_f
6	$Na_{0.81}IrO_3$	5.236 (5)	4.858 (3)	2.81
24	$Na_{0.76}IrO_3$	5.230 (4)	4.848 (2)	2.26
48	$Na_{0.84}IrO_3$	5.232 (2)	4.848 (6)	2.52

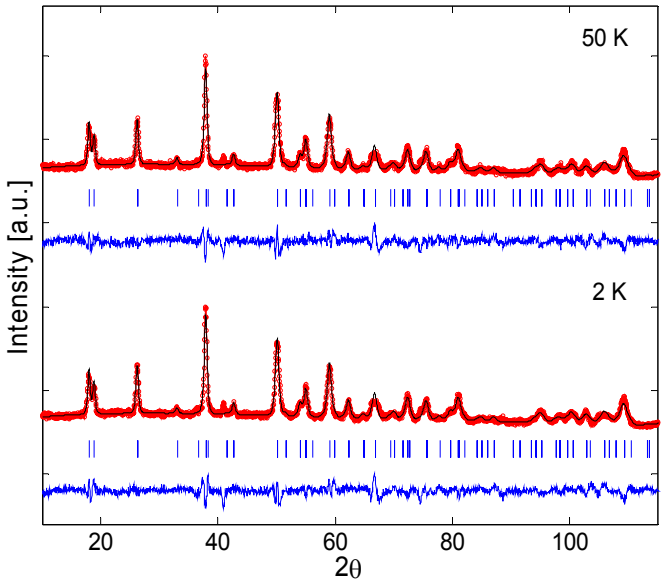

Fig. 1 Rietveld refinement with Full Prof of the neutron powder diffractogram of $Na_{0.8}IrO_3$ measured at HRPT, SINQ at 2 K and 50 K.

Table 2 Unit-cell, positional and displacement parameters for $Na_{0.8}IrO_3$ oxidized for 24h with the trigonal P-3 space group at 2 K and 50 K, obtained from Rietveld refinement of neutron powder diffraction data and at room temperature from X-ray diffraction data.

	T = 2 K	*T = 50 K*	*T = 300K*
a (Å)	5.248 (0)	5.247 (8)	5.230 (4)
c (Å)	4.754 (6)	4.755 (2)	4.848 (2)
V (Å^3)	113.405	113.412	114.865
Na1 (*0,0,0*)			
B (Å^2)	0.81 (6), 1.4 (2) anisotropic	1.49 (6), 0.9 (3) anisotropic	-0.27 (4), -0.0 (5) anisotropic
Occ	0.5 (5)	0.6 (4)	0.6 (3)
Na2 (*0,0,1/2*)			
B (Å^2)	-0.002 (7), -0.03 (7) anisotropic	-0.00 (6), 0.02 (4) anisotropic	0.01 (5), -0.02 (6) anisotropic
Occ	0.96 (1)	0.96 (4)	0.89 (8)
Ir (*1/3, 2/3, z*)			
z	-0.014	-0.01 (1)	0.00 (03)
B (Å^2)	0.01	0.2 (8)	0.36 (7)
O (x,y,z)			
x	0.62 (7)	0.62 (6)	0.67 (1)
y	0.62 (5)	0.62 (5)	0.64 (9)
z	0.216 (9)	0.216 (7)	0.17 (9)
B (Å^2)	0.98	0.83 (8)	0.30 (5)
$\mathbf{R_f}$	4.81	3.72	2.26

refinement confirms the significant reduction of the Na-content in the sample from Na_2IrO_3 to $Na_{0.8}IrO_3$ (Table 2). This change in stoichiometry goes along with the oxidation of Ir from +IV to a mixed + V/+ VI state.

Further the refinement of the neutron data shows, that the thermal parameters of sodium exhibit a high anisotropy at 2 K and 50 K along the *c*-axis. The discrepancy still observed between the calculated and observed intensities is present due to a lowered crystallinity of the specimens. Since the samples have been rinsed with water, it can be expected to have also guest water molecules within the sodium layers (Fig. 2). This can explain the measured thermal anisotropy of the sodium as well as the reduced crystallinity of the samples.

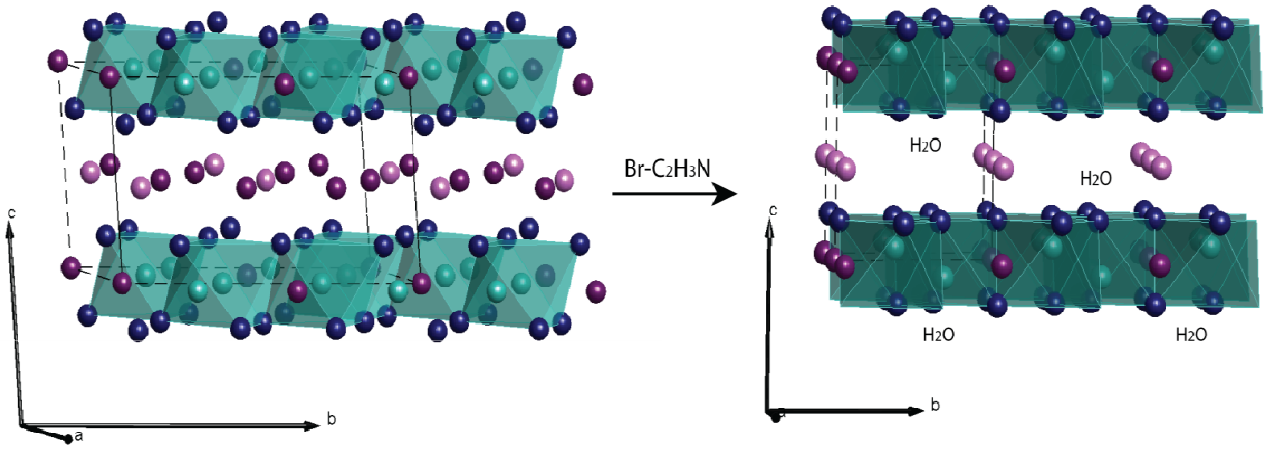

Fig. 2 Scheme of the parental compound Na_2IrO_3 (left structure) being converted to $Na_{0.8}IrO_3$ (right structure) by deintercalation of sodium plotted with SpinW [13]. The dark blue spheres illustrate the Oxygen atoms, the turquoise one, the Iridium atoms in the Oxygen tetraeders. The pink and purple spheres show the position of the two Na atoms. In $Na_{0.8}IrO_3$ these positions are also occupied by water molecules and the sodium shows a high anisotropy along the c-axis.

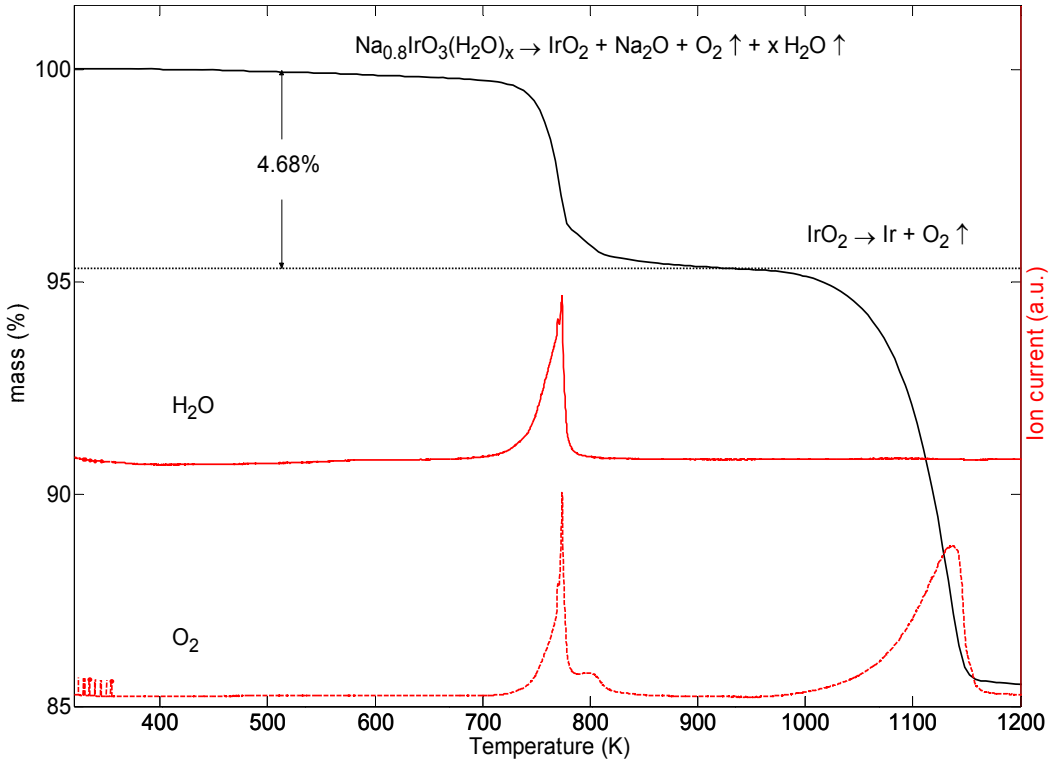

Fig. 3 Thermogravimetric measurement of $Na_{0.8}IrO_3$ deintercalated for 24 h. The black curve shows the mass change versus temperature. The red solid line shows the mass spectrometry signal corresponding to H_2O, the red dotted line corresponding to O_2.

Thermogravimetic measurements made on heating (1 K/min) in Helium (Fig. 3) are showing a decrease of the mass of 4.68% within temperature range 700-825 K. At these temperatures a release of both water and oxygen from the sample was detected by the mass spectrometer. The release of water at such high temperatures elucidates, that the water is chemically bounded in the structure (crystal water), as discussed above. Additionally, the observed oxygen release indicates decomposition of the compound to

IrO_2 and Na_2O, which was confirmed by the XRD measurements. Based on the decomposition products, the reaction equation can be written as

$$Na_{0.8}IrO_3 \cdot (H_2O)_x \rightarrow 0.4\ Na_2O + IrO_2 + 0.3\ O_2 \uparrow + x\ H_2O \uparrow$$

From the mass change the authors can roughly estimate the amount of crystal water, to be 0.97% of the mass, which is equal to 0.14 mol. In a second reaction step starting at 1,000 K, the IrO_2 is reduced to Ir and O_2. The attempt to increase the crystallinity of the samples, by annealing below the decomposition temperature at 723 K for 24 h resulted in the decomposition as well.

3.2 Magnetic Properties

Magnetic susceptibility measurements of all deintercalated samples showed similar magnetic properties. Instead of an antiferromagnetic transition present in the parent phase at 15 K, all specimens show a paramagnetic behavior down to 2 K. For the sake of clarity only the data for the 24 h-deintecalated sample are plotted in Fig. 4. The linear fit of the inverse susceptibility between 250 K and 300 K gives an effective magnetic moment $\mu_{\text{eff}} = 1.84\ \mu_B$ which is consistent with a mixture of iridium on fifth and sixth oxidation states, with the expected effective moments of 2.82 μ_B for Ir(V) and 1.73 μ_B for Ir(VI). However the effective moment found in all three samples is smaller than expected for the overall stoichiometry found by structural studies. This can be caused by a small intrinsic itinerant moment, but considering the low temperature Curie tail in all measured samples, the reduced moment is probably caused by small proportion of paramagnetic impurities. With a Curie Weiss Temperature θ of -1,347 K, the system seems to be highly frustrated. However the high Curie temperature could be partially caused by the change of the moment with temperature, since the material shows semiconducting behavior.

As it is listed in Table 3, the samples deintercalated for 6 h and 48 h respectively, show a similar magnetic moment and θ, supporting the result, that within the time frame of 6 h to 48 h no further significant amount of sodium is removed. Since the Curie temperature is very high in all the samples, and the susceptibility was measured up to 300 K, the effective magnetic moment cannot be properly fit, which can explain the small difference within the samples, assuming the samples to have very similar stoichiometry.

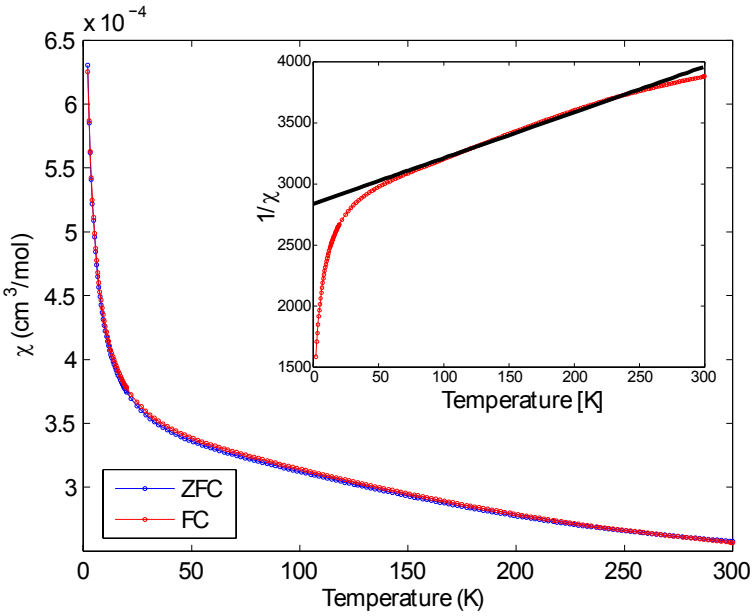

Fig. 4 Susceptibility data of $Na_{0.8}IrO_3$, deintercalated for 24 h, measured at 1 T. The inset shows the fitted inverse susceptibility.

Table 3 The magnetic moment μ_{eff} and Curie Weiss temperature θ of Na_2IrO_3 deintercalated for 6 h, 24 h and 48 h.

Na_2IrO_3 deintercalated for	μ_{eff} (μ_B)	θ (K)	C ($cm^3K/mol/Oe$)
6 h	1.95	-1,559	0.4785
24 h	1.84	-1,347	0.4244
48 h	1.68	-1,186	0.3545

Fig. 5 For table of contents only: By hole doping Na_2IrO_3 on the sodium site, it was possible to synthesize $Na_{0.8}IrO_3$, an Iridate with higher oxidation state than +IV. The sodium is removed by the oxidizing Bromine/acetonitrile solution and is partially replaced by water molecules. While the honeycomb structure remains, the symmetry of the compound changes from C2/c to P-3. This new honeycomb-compound shows a paramagnetic behavior and is a semiconductor.

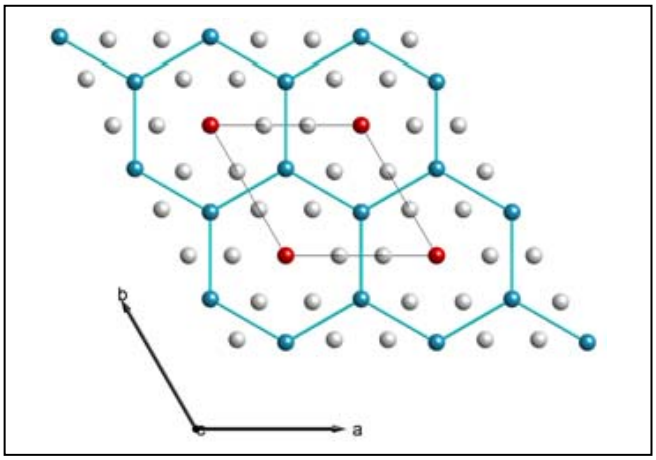

Fig. 5 The new honeycomb compound $Na_{0.8}IrO_3$ with P-3 symmetry.

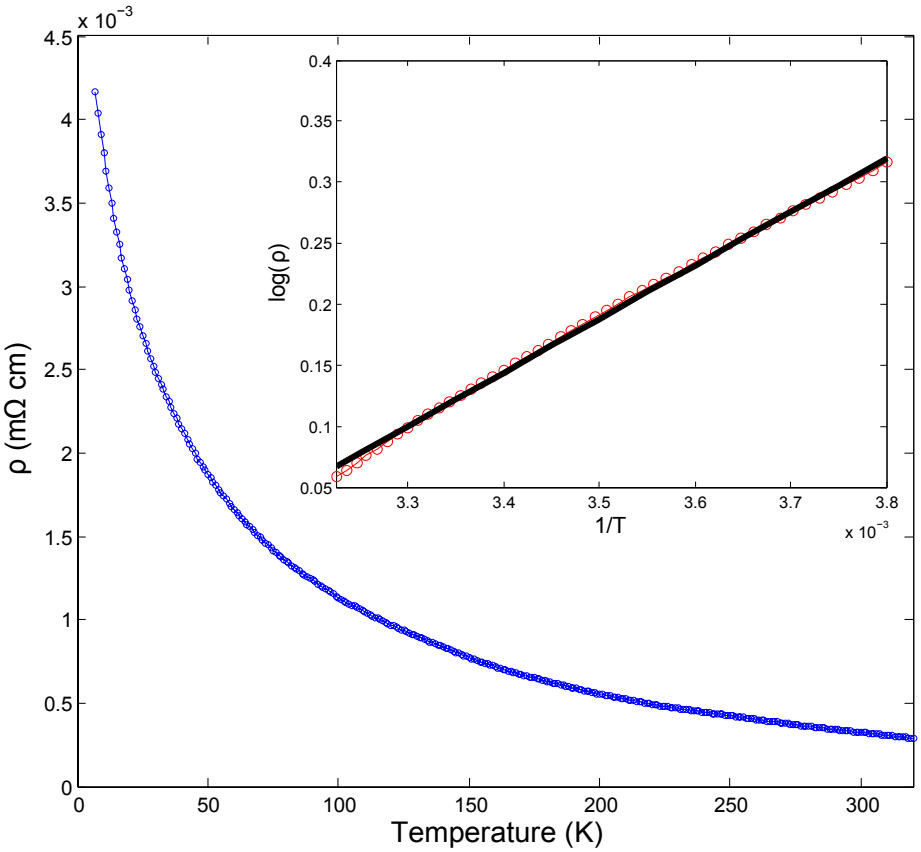

Fig. 6 Resistivity of $Na_{0.8}IrO_3$ deintercalated for 24 h, indicating a non-metallic behavior. The inset shows the linear fit of log(p) vs 1/T with the Arrhenius law $\sigma(T) = \sigma_0 e^{(-E_a/kT)^m}$ with m = 1.

3.3 Transport Measurements

Consistently with the absence of magnetic ordering or structural phase transition at low temperature, the heat capacity measurements show no peak in the measured temperature range from 2 K up to 300 K. As stated in the Introduction, the strong spin orbit coupling of Iridium in the oxidation state + IV can lead to the Mott insulator state in several iridates. This state is observed in the parental phase Na_2IrO_3. As discussed before, the deintercalation leads to the oxidation of the Ir(+IV) to a mixed Ir(+V/+VI) state, changing also the ground state of $Na_{0.8}IrO_3$. Bremholm et al., found the high pressure $NaIrO_3$ containing pentavalent Iridium, has a nonmetallic behavior with a variable range hopping [12]. The resistivity measurements of $Na_{0.8}IrO_3$ showed a much lower resistivity of 0.0028 Ω cm at room temperature and 0.0427 Ω cm at 2 K than found in $NaIrO_3$ (400 Ω cm at 2 K). Furthermore a semiconductor behavior was revealed (Fig. 6) and could be fitted in the high temperature region between 260 K and 310 K by the Arrhenius law $\sigma(T) = \sigma_0 e^{(-E_a/kT)^m}$ with m = 1, with a band gap of 0.083 eV.

4. Conclusion

In conclusion the authors could present a new method to synthesize a compound with Iridum at higher oxidations state than + IV at ambient pressure. The deintercalation of sodium from Na_2IrO_3 results in a significant reduction of the sodium content enabling a new way of oxidizing Ir(IV) Ir(V) and Ir(VI). This goes along with the formation of a new compound with a trigonal crystal structure (space group P-3). Independent of the time within the chosen timeframe of 6 h to 48 h, the deintercalation process reached its "equilibrium" resulting in the same final stoichiometry of $Na_{0.8}IrO_3$. The authors could show that the lattice incorporates small amount of water molecules during the rinsing process. With the deintercalation and the resulting oxidization of the Iridium from +IV to a mixed +V/+VI state, the samples show no magnetic ordering down to 2 K. Furthermore the ground state changes from a Mott insulating state to a semiconductor behavior with a band gap of 0.083 eV.

Author Contributions

The manuscript was written through contributions of all authors. All authors have given approval to the final version of the manuscript.

Acknowledgment

This work is based on experiments performed at the Swiss spallation neutron source SINQ, Paul Scherrer Institute, Villigen, Switzerland. The authors acknowledge the allocation of the beam time at the HRPT diffractometer of the Laboratory for Neutron Scattering and Imaging (PSI, Switzerland). The authors thank SNF Sinergia project "Mott physics beyond Heisenberg model" for the support of this study.

References

[1] Kim, B., Jin, H., Moon, S., Kim, J. Y., Park, B. G., Leem, C., Yu, J., Noh, T., and et al.. 2008. "Novel J_{eff} = 1/2 Mott State Induced by Relativistic Spin-Orbit Coupling in Sr_2IrO_4." *Phys. Rev. Lett.*101: 1-4.

[2] Kim, J., Casa, D., Upton, M. H., Gog, T., Kim, Y. J., Mitchell, J. F., Veenendaal, M., Daghofer, M., and et al.. 2012. "Magnetic Excitation Spectra of Sr_2IrO_4 Probed by Resonant Inelastic X-Ray Scattering: Establishing Links to Cuprate Superconductors." *Phys. Rev. Lett.*108: 177003.

[3] Singh, Y., and Gegenwart, P. 2010. "Antiferromagnetic Mott Insulating State in Single Crystals of the Honeycomb Lattice Material Na_2IrO_3." *Phys. Rev. B*82: 064412.

[4] Chaloupka, J., Jackeli, G., and Khaliullin, G. 2010. "Kitaev-Heisenberg Model on a Honeycomb Lattice: Possible Exotic Phases in Iridium Oxides A_2IrO_3." *Phys. Rev. Lett.*105: 027204.

[5] Choi, S. K., Coldea, R., Kolmogorov, A. N., Lancaster, T., Mazin, I. I., Blundell, S. J., Radaelli, P. G., Singh, Y., and et al.. 2012. "Spin Waves and Revised Crystal Structure of Honeycomb Iridate Na_2IrO_3." *Phys. Rev. Lett.*108: 127204.

[6] Kitaev, A. 2006. "Anyons in an Exactly Solved Model

and Beyond." *Annals of Physics*321: 2

[7] Reuther, J., Thomale, R., Trebst, S. 2011. "Finite-temperaturephase Diagram of the Heisenberg-Kitaev Model." *Phys. Rev. B*84: 100406.

[8] Mei, J. W. 2012. "Possible Fermi Liquid in the Lightly Doped Kitaev Spin Liquid." *Phys. Rev. Lett.*108: 227207.

[9] You, Y. Z., Kimchi, I., Vishwanath, A. 2012. "Doping a Spin-orbit Mott Insulator: Topological Superconductivity from the Kitaev-Heisenberg Model and Possible Application to $(Na_2/Li_2)IrO_3$." *Phys. Rev. B*86: 085145.

[10] Takada, K., Sakurai, H., Takayama-Muromachi, E., Izumi, F., Dilanian, R. A., and Sasaki, T. 2003. "Superconductivity in Two- dimensional CoO_2 Layers." *Nature*422: 53-5.

[11] Fischer, P., Frey, G., Koch, M., Ko, M., Pomjakushin, V., Schefer, J., Thut, R., Schlumpf, N. and et al.. 2000. "High-resolution Powder Diffractometer HRPT for Thermal Neutrons at SINQ." *Phys. B*276: 146-7.

[12] Bremholm, M., Dutton, S. E., Stephens, P. W., and Cava, R. J. 2011. "$NaIrO_3$—A Pentavalent Post-Perovskite." *J. Solid State Chem.*184: 601-7.

[13] Toth, S., and Lake, B. 2015. "Linear Spin Wave Theory for Single-Q Incommensurate Magnetic Structures." *J. Phys. Condens. Matter* 27: 166002.